

SVT-Net: Super Light-Weight Sparse Voxel Transformer for Large Scale Place Recognition

Zhaoxin Fan

Renmin University of China

fanzhaoxin@ruc.edu.cn

Hongyan Liu

Tsinghua University

liuhh@sem.tsinghua.edu.cn

Jun He*

Renmin University of China

he_jun@ruc.edu.cn

Zhenbo Song

Nanjing University of Science and Technology

songzb@njust.edu.cn

Zhiwu Lu

Renmin University of China

luzhiwu@ruc.edu.cn

Xiaoyong Du

Renmin University of China

duyong@ruc.edu.cn

Abstract

Point cloud-based large scale place recognition is fundamental for many applications like Simultaneous Localization and Mapping (SLAM). Although many models have been proposed and have achieved good performance by learning short-range local features, long-range contextual properties have often been neglected. Moreover, the model size has also become a bottleneck for their wide applications. To overcome these challenges, we propose a super light-weight network model termed SVT-Net for large scale place recognition. Specifically, on top of the highly efficient 3D Sparse Convolution (SP-Conv), an Atom-based Sparse Voxel Transformer (ASVT) and a Cluster-based Sparse Voxel Transformer (CSVT) are proposed to learn both short-range local features and long-range contextual features in this model. Consisting of ASVT and CSVT, SVT-Net can achieve state-of-the-art on benchmark datasets in terms of both accuracy and speed with a super-light model size (0.9M). Meanwhile, two simplified versions of SVT-Net are introduced, which also achieve state-of-the-art and further reduce the model size to 0.8M and 0.4M respectively.

1 Introduction

Large scale place recognition and localization is fundamental for a wide range of applications like Simultaneous Localization and Mapping (SLAM) [27, 28], autonomous driving [21, 11], robot navigation [29, 33], etc. For example, the place recognition result is used as a signal for loop-closure [4] in SLAM systems, when GPS signal is not available. A line of works [22, 13, 43] have chosen to use images for place recognition, which have shown promising performance. However, images are sensitive to illumination, weather change, diurnal variation, etc, making models based on them unstable and unreliable. Besides, due to lack of depth information, image based methods are hard to fully understand the scene and are easily cheated by planar puzzles.

To tackle these challenges, a feasible solution is replacing images with point clouds collected by LiDAR. Scenes represented by point clouds are inherently invariant to illumination and weather changes and contain accurate and detailed 3D information meanwhile. Recently, a range of deep learning models [36, 44, 35, 24, 8, 41, 20] that utilize point clouds for place recognition have been proposed. Figure 1 (Left) illustrates the common pipeline of these point cloud based place recognition

*Corresponding author

methods. For a large scale region, a database of LiDAR scans tagged with UTM coordinates acquired from GPS/INS readings are constructed in advance. When a query scan is collected by the LiDAR from scratch, the most similar point cloud to the query scan is retrieved from the database to determine where the location of the query scan is.

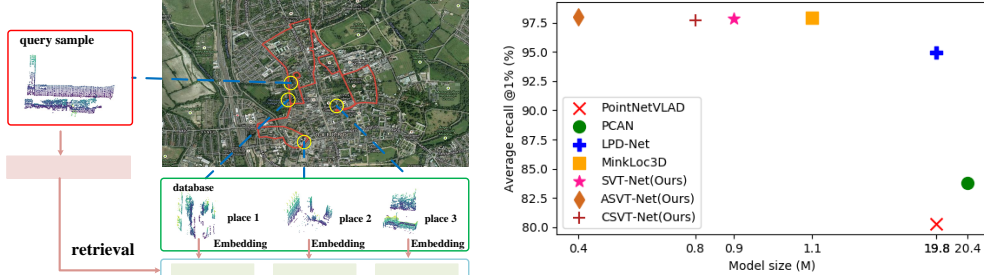


Figure 1: (Left) Pipeline of point cloud based place recognition. (Right) Model size and accuracy.

To achieve accurate retrieval, a powerful deep learning model is needed to learn discriminative scene descriptors or embeddings of point clouds. Learning powerful scene descriptors is the key to the recognition task. However, we observe that, when learning scene descriptors, most of previous methods only consider how to better extract short range local features, while the equally important long range contextual properties have long been neglected. And we argue that lacking awareness of long range contextual properties, power of final descriptors would be greatly limited. Besides, we also notice that model size has become a bottleneck for further performance improving and practical popularizing. More specifically, in most of SLAM or robot navigation systems, the available memory is tight. Therefore, the smaller the model size, the more favorable the model is. Models with small size can be deployed on more hardware products and can serve for more scenarios. Therefore, designing light-weight descriptor learning models with small size and fast running time is necessary.

Motivated by the above observations, we propose a novel super light-weight network named SVT-Net in this paper. In this model, each point cloud is first voxelized into sparse voxel representations to characterize structured information of the scene. Then, we choose the light weight 3D Sparse Convolution (SP-Conv) [5] as our basic unit to extract local features owing to its flexibility and powerful local feature learning ability. However, simply stacking SP-Conv layers may ignore long range contextual properties. Therefore, inspired by recently proposed Vision Transformer Networks [7, 40], we propose two kinds of Sparse Voxel Transformers (SVTs) named Atom-based Sparse Voxel Transformer (ASVT) and Cluster-based Sparse Voxel Transformer (CSV) respectively on top of SP-Conv layers. ASVT and CSV can extract long range contextual features implicit in the sparse voxel representation from two perspectives: attending on different key atoms and clustering different key regions in the feature space, thereby helping to obtain more discriminative descriptors through interacting different atoms and different clusters respectively. As SP-Conv only conducts convolution operation on non-empty voxels, computation is efficient and flexible, and so do the two SVTs built upon it. Thanks to the strong capabilities of the two SVTs, our proposed model can learn sufficiently powerful descriptors from an extremely shallow network architecture. Meanwhile, model size of SVT-Net is very small as shown in Figure 1 (Right). Experiment result shows that though small, SVT-Net achieves state-of-the-art performance in terms of both accuracy and speed on Oxford RobotCar dataset [26] and three in-house datasets [36]. What's more, to further increase speed and reduce model size, we develop two simplified version of SVT-Net: ASVT-Net and CSV-Net, which can also achieve state-of-the-art performances with further reduced model sizes of only 0.8M and 0.4M respectively.

Our main contributions are summarized below. 1) We propose a novel light-weight point cloud based place recognition model named SVT-Net as well as two simplified versions: ASVT-Net and CSV-Net, which all achieve state-of-the-art performance in terms of both accuracy and speed with a extremely small model size. 2) We propose Atom-based Sparse Voxel Transformer(ASVT) and Cluster-based Sparse Voxel Transformer(CSV) for learning long range contextual features hidden in point clouds. To the best of our knowledge, we are the first to propose Transformers for sparse voxel representations. 3) We have conducted extensive quantitative and qualitative experiments to verify the effectiveness and efficiency of our proposed models and analyse what the two proposed Transformers actually learn.

2 Related Work

2.1 Large Scale Place Recognition

Large scale place recognition has been long interested in by researchers. In early years, hand-craft features like SIFT [25], SURF [2] and ORB [34] extracted from images are used on this task [10, 9, 18]. Though simple, hand-craft features own limited powers. Therefore, with the development of deep learning, automatically learning features from raw input becomes more popular. A typical deep learning method for place recognition is NetVLAD [1], which learns global descriptors by clustering CNN features into several different visual words. Then, a variety of following works [43, 15] are proposed to improve it and have achieved promising results. However, though much more powerful compared to hand-craft features, learned image features still suffer from their sensitivity towards illumination, weather change, diurnal variation, etc.

Recently, utilizing point clouds for large scale place recognition has attracted more attention owing to point cloud's robustness towards environmental changes. PointNetVLAD [36] is a pioneering work. It first uses models PointNet [31] and NetVLAD [1] to learn global descriptors. Then a K-Nearest-Neighbors (KNNs) algorithm is used for retrieval and recognition. Later, Zhang and Xiao [44] propose a contextual aware attention mechanism to help the model learn stronger local features in their proposed model PCAN. Models DAGC [35], SRNet [8] and LPD-Net [24] proposed in recent two years all use Graph Convolutional Networks (GCNs) to capture local features. More recently, a PointOE module is introduced in SOE-Net [41], which encodes local features from eight orientations to improve place recognition performance. The above mentioned methods all learn point cloud features by taking non-structure point-wise representations as input, which requires a huge model with large amount of parameters to learn reliable features. In contrast, authors of Minloc3D [20] propose to use sparse voxel representations as input and build a simple Feature Pyramid Network like architecture for learning point cloud descriptors, which becomes the current state-of-the-art. Model size of Minloc3D has been significantly reduced. However, it neglects the importance of long range contextual properties hidden in the point cloud. In our work, we also use sparse voxel representations as input. But we further propose two Sparse Voxel Tranformers (SVTs) to learn long range contextual properties. And thanks to the strong capability of the two SVTs, the model size of our work is further reduced.

2.2 Vision Transformers

Transformer [38] is originally proposed for natural language processing (NLP) tasks [6, 16, 42, 19, 3]. Self-attention mechanism is the core of Transformer, owing to its ability of capturing long range contextual information. At present, Transformer has become the most important basic module in NLP field. Inspired by the great success of Transformer in the field of NLP, researchers gradually begin to think whether self-attention mechanism can also play a role in the field of computer vision.

Therefore, Vision Transformer (ViT) [7] is proposed recently. It adopts the idea of self-attention and divides images to 16x16 visual words. In this way, images can be processed like nature language. Then, a variety of following works [40, 39, 23] are proposed to improve it. For example, Wu et al. [40] propose Visual Transformer (VT), which elegantly projects image features into tokens and processes these tokens by means of the classic Transformer [38], reducing computational cost greatly. In PVT [39], a FPN like structure is introduced to cope with dense prediction tasks. A hierarchical architecture is presented in Swin-Transformer [23]. By limiting self attention to non overlapping local windows, higher efficiency can be achieved in this model. More recently, Jiang et al. [17] successfully employ vision Transformers in GANs. For a more comprehensive introduction of Vision Transformers on 2D images, we refer readers to [14]. The above introduced vision Transformers are all designed for processing images. For Transformers to process point cloud, there are only a few works [45, 12], which means that the 3D vision of Transformer is still under-explored. In this paper, we propose two kinds of Transformers that can be used for processing point clouds with sparse voxel representations. To the best of our knowledge, this is the first work that designs Sparse Voxel Transformers for point clouds.

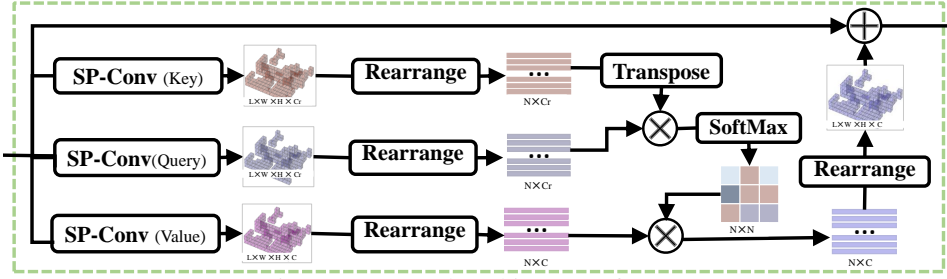


Figure 2: Network architecture of ASVT.

3 Methodology

3.1 Problem Statement

Let $M_r = \{m_i | i = 1, 2, \dots, M\}$ be a database of pre-defined 3D submaps (represented as point clouds), and Q be a query point cloud scan. The place recognition problem is defined as retrieving a submap m_s from M_r with the goal of m_s is the closest one to Q . To achieve accurate retrieving, a deep learning model $F(\cdot)$ that can embed all point clouds into discriminative global descriptors, e.g. $Q \rightarrow f_q \in R^d$, is required so that a following KNNs algorithm can be used for finding m_s . To meet the goal, we choose to use the sparse voxel presentation of point cloud as input and choose 3D Sparse Convolution (SP-Conv) [5] as basic unit to build the deep learning model. To employ SP-Conv [5], we first voxelize all point clouds into sparse voxel representations, e.g. $Q \rightarrow Q^v \in R^{L \times W \times H \times 1}$, where for each voxel, 1 means that it is occupied by any points in Q , called non-empty voxel, and otherwise 0, called empty voxel. SP-Conv operation is only conducted on non-empty voxels. Hence, it is very efficient and flexible. Next, we will introduce the proposed two transformers: the Atom-based Sparse Voxel Transformer (ASVT) and the Cluster-based Voxel Transformer (CSVT) respectively. And then, the overall network architecture of SVT-Net as well as network architectures of the two simplified versions (ASVT-Net and CSVT-Net) will be introduced in detail. The loss function will be presented finally.

3.2 Atom-based Sparse Voxel Transformer

As mentioned before, simply stacking SP-Convs can only learn local information from nearby voxels. To capture long range contextual properties hidden in point cloud, we design ASVT, which adopts the idea of self-attention to aggregate information from both nearby and far-away voxels. In ASVT, we define each individual voxel as an atom. During processing, each atom should be interacted with all other atoms according to the learned per-atom contributions. By doing so, different key atoms could be attended by other atoms so that both local relationship of nearby atoms and long range contextual relationship of far way atoms will be learned. Note that learning such kind of long range contextual relationship is very important for the model. For example, in a scene, assume there are two atoms that belong to different instances of the same category. If only SP-Conv is used, the "same-category" information may be ignored due to the small receptive field. While if ASVT is added to learn such kind of information, the model can better encode what the scene describes. Hence the final global descriptor would be more powerful. The architecture of ASVT is illustrated in Figure 2.

Let $X_{in} \in R^{L \times W \times H \times C}$ be the input sparse voxel features learned by SP-Convs (SP-voxel features for simplicity). We first learn the sparse voxel values (SP-values for simplicity) $X_v \in R^{L \times W \times H \times C}$, SP-queries $X_q \in R^{L \times W \times H \times C_r}$, and SP-keys $X_k \in R^{L \times W \times H \times C_r}$ through three different SP-Convs respectively:

$$X_v = SPCconv(X_{in}), X_q = SPCconv(X_{in}), X_k = SPCconv(X_{in}) \quad (1)$$

where we often set $C_r < C$ to reduce computational cost in later steps. That is to say, the dimension of SP-queries and SP-keys are reduced from C to C_r for efficiency. After that, SP-voxel features of SP-values (SP-queries/keys) are rearranged to a tensor of $N \times C$ ($N \times C_r$), where N is the number of non-empty voxels.

Then, we use X_q and X_k to calculate the SP-attention map S :

$$S = softmax(X_q \cdot X_k^T) \quad (2)$$

where $S \in R^{N \times N}$ encodes the contribution relationship of each atom with all the other atoms. In the following attending operation, these relationships will contribute to aggregating both short range local information and long range contextual information by interacting atoms. The attending operation can be summarized as:

$$X_s = SPCconv(S \cdot X_v) \quad (3)$$

where $X_s \in R^{N \times C}$ is called atom-attended SP-voxel features. In X_s , features of each atom x_i have adaptively accepted contributions from all the other atoms according to the implicit mode hidden in S . Thus meaningful contextual and semantic information can be represented in X_s to describe the scene.

Finally, we rearrange X_s back to sparse voxel representations with a dimension of $L \times W \times H \times C$ and regard it as a residential term. The final ASVT feature is defined as the sum of X_{in} and X_s :

$$X_{asvt} = X_{in} + X_s \quad (4)$$

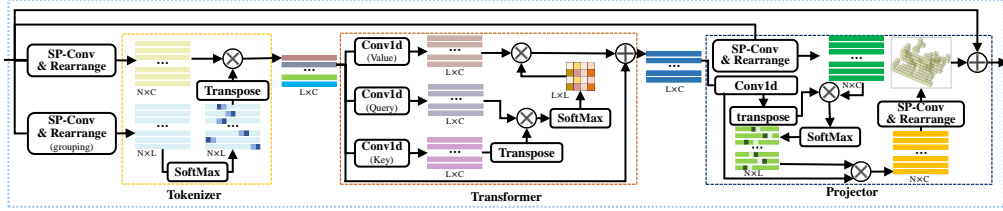


Figure 3: Network architecture of CSVT.

3.3 Cluster-based Sparse Voxel Transformer

Another observation we find is that in the sparse voxel representation, some atoms may share the same characteristics. For example, atoms of a wall always form a plane like structure, while atoms of a flower bed easily form a cylinder like structure. This means that atoms can actually cluster into different clusters according to their geometric or semantic characteristics, and the long range contextual properties can also be extracted from the perspective of interacting between these clusters. Motivated by this intuition, we propose CSVT, which is illustrated in Figure 3. As shown in the figure, CSVT consists of three component, a Tokenizer module, a Transformer module and a Projector module.

The Tokenizer module is used to transform the input SP-voxel features into tokens, where each token represents a cluster in the latent space. We again define $X_{in} \in R^{L \times W \times H \times C}$ as the initial SP-voxel features. To achieve the goals of the tokenizer, we first use a SP-Conv operation followed by a rearrange operation to generate a grouping map $X_g \in R^{N \times L}$:

$$X_g = \text{softmax}(RE(SPCconv(X_{in}))) \quad (5)$$

where RE is the rearrange operation. L is the number of tokens we choose to generate. X_g stores the probabilities of each voxel belonging to each token. Therefore, we can use X_g to capture representations of tokens as grouping different tokens into different clusters:

$$T = X_g^T \cdot SPCconv(X_{in}) \quad (6)$$

where $T \in R^{L \times C}$ denotes representations of L tokens with each of them described by C features.

The Transformer module is then used to learn long range properties among different clusters through interacting these tokens. First, we generate values, keys, and queries using shared convolution kernel Conv1d :

$$T_v = \text{Conv1d}(T), T_q = \text{Conv1d}(T), T_k = \text{Conv1d}(T) \quad (7)$$

Then, tokens are interacted with each other through the following attention operation:

$$T_s = T + \text{Conv1d}(\text{softmax}(T_q \cdot T_k^T) \cdot T_v) \quad (8)$$

where $T_s \in R^{L \times C}$ is the attended tokens. Through the Transformer module, relationship between different clusters are learned to characterize the distribution characteristics of the scene with high quality. For example, the final descriptor may memorize that there is a rectangular building in the

scene 5 meters away from a cylindrical building, or remember that there is a spherical building behind a slender tree.

The Projector module is then used to project token features back to the sparse voxel representations. Specifically, we use T_s to calculate a projection map $M_p \in R^{N \times L}$:

$$T_p = \text{Conv1d}(T_s) \quad (9)$$

$$M_p = \text{softmax}(\text{RE}(\text{SPConv}(X_{in})) \cdot T_p^T) \quad (10)$$

Then, the projection operation is defined as:

$$X_s = \text{SPConv}(M_p \cdot T_p) \quad (11)$$

Again, we rearrange X_s back to sparse voxel representations with a dimension of $L \times W \times H \times C$ and regard it as a residual term. The final CSVT feature is defined as:

$$X_{csvt} = X_{in} + X_s \quad (12)$$

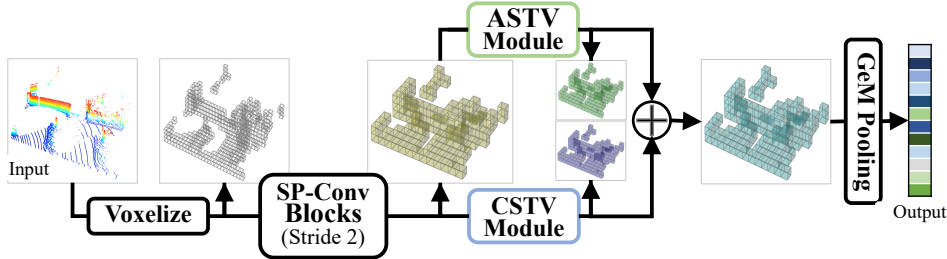


Figure 4: Pipeline of SVT-Net.

3.4 Network Architecture

The overall architecture of SVT-Net is built upon the above introduced ASVT and CSVT as well as the 3D Sparse Convolution (SP-Conv). Specifically, as shown in Figure 4. The initial sparse voxel representation is fed into the first SP-Conv layer with an output dimension of 32 to learn initial sparse voxel features. Then a SP-Res-Block consisting of two SP-conv layers with skip connection is used to enhance learned features and increase the feature dimension to 64. Next, another SP-conv layer is used to increase the feature dimension to the final descriptor's dimension d . After that, the SP voxel features are fed into two branches for learning the ASVT feature and the CSVT feature using the two proposed Sparse Voxel Transformers (SVTs) respectively. Then, the learned ASVT feature and CSVT feature are fused by directly adding them together. Finally, the final global descriptor is calculated using a GeM Pooling operation [32, 20]. Detailed information about network architecture can be found in **supplementary materials**. Thanks to the strong power of ASVT and CSVT, our proposed model SVT-Net can achieve superior performance compared to previous methods, even though our network architecture is simpler and smaller. Note that ASVT and CSVT can also be individually utilized in different networks. Therefore, we propose two simplified versions of SVT-Net: ASVT-Net and CSVT-Net, by eliminating the ASVT module and CSVT module, respectively. According to experimental results, both ASVT-Net and CSVT-Net also achieve state-of-the-art performance but further reduce model size for a large margin.

3.5 Loss Function

To train our model, we adopt the following triplet loss as proposed in [20]:

$$L(f_i, f_i^p, f_i^n) = \max\{d(f_i, f_i^p) - d(f_i, f_i^n) + m, 0\} \quad (13)$$

where f_i is the descriptor of the query scan, f_i^p and f_i^n are descriptors of positive sample and negative sample respectively, and m is a margin. $d(x, y)$ means the Euclidean distance between x and y . To build informative triplets, we use batch-hard negative mining following [20].

After the network is trained, all point clouds are embedded into descriptors using the model. And we use the KNNs algorithm to find m_s in the database, which is the closest one to query scan Q .

Table 1: Comparison with the state-of-the-art methods under the baseline setting.

Method	Average recall at top-1% (%)				Average recall at top-1 (%)			
	Oxford	U.S.	R.A.	B.D.	Oxford	U.S.	R.A.	B.D.
PointNetVLAD	80.3	72.6	60.3	65.3	-	-	-	-
PCAN	83.8	79.1	71.2	66.8	-	-	-	-
DAGC	87.5	83.5	75.7	71.2	-	-	-	-
SOE-Net	96.4	93.2	91.5	88.5	-	-	-	-
SR-Net	94.6	94.3	89.2	83.5	86.8	86.8	80.2	77.3
LPD-Net	94.9	96.0	90.5	89.1	86.3	87.0	83.1	82.3
Minkloc3D	97.9	95.0	91.2	88.5	93.0	86.7	80.4	81.5
SVT-Net(Ours)	97.8	96.5	92.7	90.7	93.7	90.1	84.3	85.5
ASVT-Net(Ours)	98.0	96.1	92.0	88.4	93.9	87.9	83.3	82.3
CSVT-Net(Ours)	97.7	95.5	92.3	89.5	93.1	88.3	82.7	83.3

4 Experiments

4.1 Datasets and Metrics

We use the benchmark datasets proposed by [36] to evaluate our methods. The benchmark contains four datasets: one outdoor dataset named Oxford generated from Oxford RobotCar [26] and three in-house datasets: university sector (U.S.), residential area (R.A.) and business district (B.D.). The benchmark contains 21,711, 400, 320, 200 submaps for training and 3,030, 80, 75, 200 submaps for testing for Oxford., U.S., R.A. and B.D. respectively. Ground points of each submaps are removed and finally each point cloud contains 4096 points. In training, point clouds are regarded as correct matches if they are at maximum 10m apart and wrong matches if they are at least 50m apart. In testing, the retrieved point cloud is regarded as a correct match if the distance is within 25m between the retrieved point cloud and the query scan. Following previous works [36, 44, 35, 24, 8, 41, 20], we choose average recall at top N as our metric, which means if one of the top N retrieved submaps matches the query scan, we regard the retrieval is correct. Among top “N”, average recall at top 1% and average recall at top 1 are most frequently reported.

4.2 Implementation Details

In all experiments, we voxelize 3D point coordinates with 0.01 quantization step. The voxelization and the following SP-Conv operation are performed by the MinkowskiEngine auto differentiation library [5]. The dimension of the final descriptor is set to 256. The number of tokens L is set to 8. In ASVT, dimension of X_q and X_k is reduced by a factor of 8 from the input, i.e. from 256 \rightarrow 32. The margin m in the loss function is set to 0.2. The same as in [20], to prevent embedding collapse in early epochs of training, we use a dynamic batch sizing strategy. During training, we count the number of active triplets, when it falls below 70% of the current batch size, the batch is increased by 40% until the maximum size of 256 elements is reached. Following previous work, we train two versions of models: baseline model and refined model. The baseline model is trained only using the training set of Oxford dataset, and the refined model is trained by adding the training set of U.S. and R.A. (Note that training set of B.D. is not added). In the baseline setting, the initial batch size is 32 and the initial learning rate is 10^{-3} . The model is trained for 40 epochs and the learning rate is decayed by 10 at the end of the 30th epoch. The refined model is trained with an initial batch size of 16 and an initial learning rate of 10^{-3} . The model is trained for 80 epochs and the learning rate is decayed by 10 at the end of the 60th epoch. The model is implemented by pytorch [30] and optimized by Adam optimizer. Random jitter, random translation, random points removal and random erasing augmentation are adopted for data augmentation during training. All experiments are performed on a Tesla V100 GPU with a memory of 32G.

4.3 Main Results

In this section, we would like to experimentally answer the following questions: Can SVT-Net surpass existing methods in terms of accuracy ? Does SVT-Net really meet the requirements of super light-weight in terms of model size and inference speed? And what features have ASVT and CCSV learned to help improve performance?

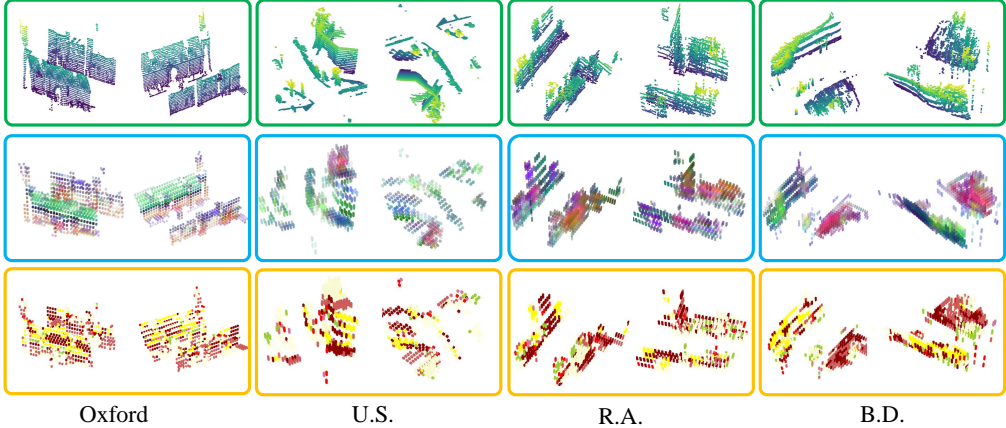


Figure 5: Visualization of what ASVT and CSVT have learned.

Accuracy: To verify the effectiveness of our method, we compare our models with PointNetVLAD [36], PCAN [44], DAGC [35], SR-Net [8], LPD-Net [24], SOE-Net [41] and Minkloc3D [20]. In Table 1, we show the results of all methods on the baseline setting. It can be found that SVT-Net significantly outperforms all state-of-the-art methods, especially for the average recall at top 1 metric on U.S., R.A., and B.D., where SVT-Net wins for 3.4%, 3.9%, 4% compared to Minkloc3D respectively. Compared to SVT-Net, performances of ASVT-Net and CSVT-Net drop to some extent. However, their performances still largely outperform the previous best model Minkloc3D. We contribute the accuracy gain to the two novel SVTs we design. Note that Minkloc3D is also built upon SP-Conv and shares the same loss function as our model, while its performance is not as excellent as our models, which further confirms the superiority of our two proposed SVTs. Recall curves of the baseline setting can be found in **supplementary materials**. For a comprehensive comparison, we also show the results of all models at the refined setting in **supplementary materials**. We find that at the refined setting, our models still significantly outperform all models except Minkloc3D. In fact, our models still performs better than Minkloc3D in most cases, although only by a small margin. The difference between our three models becomes narrow. We attribute this to that all models have reached the performance upper bound.

Table 2: Efficiency comparison.

Method	Time	Parameters
PointNetVLAD	-	19.8M
PCAN	-	20.4M
LPD-Net	-	19.8M
Minkloc3D	12.16ms	1.1M
SVT-Net(Ours)	12.97ms	0.9M
ASVT-Net(Ours)	11.04ms	0.4M
CSVT-Net(Ours)	11.75ms	0.8M

accuracy at the baseline setting. The ability of significantly improving accuracy under the condition of drastically reduced parameters has further fully demonstrated the superiority of our two SVTs. For speed, compared to the current fastest model Minkloc3D, SVT-Net only add ignorable additional inference time. And both ASVT-Net and CSVT-Net run faster than Minkloc3D. In a word, our models are good enough in terms of both model size and speed.

What transformers have learned: One may be interested in what ASVT and CSVT have learned that could make our models so elegant. To explore this question, we show some visualization results in Figure 5. The first row shows the original point clouds randomly selected from Oxford, U.S., R.A. and B.D respectively. In the second row, we visualize the features of each non-empty voxel after ASVT using T-SNE [37]. Different colors represent different distribution of these features in the feature space. It can be seen that by interacting each atom with all the others, the model indeed learns the relationship between atoms. Specifically, it is obvious that nearby atoms share the same

Table 3: Results of ablation study for our SVT-Net.

Method	Average recall at top-1% (%)				Average recall at top-1 (%)			
	Oxford	U.S.	R.A.	B.D.	Oxford	U.S.	R.A.	B.D.
A: L=4, d=256, add	97.9	96.4	92.5	89.0	93.7	89.0	83.9	82.5
B: L=6, d=256, add	98.0	96.2	92.3	90.1	93.8	88.3	83.7	84.4
C: L=10, d=256, add	97.9	96.2	92.0	89.4	93.8	87.2	83.3	83.5
D: L=8, d=128, add	97.8	95.2	92.0	89.0	93.3	88.9	81.9	82.5
E: L=8, d=384, add	98.2	94.8	92.5	89	94.4	86.9	84.9	83.7
F: L=8, d=512, add	98.0	97.3	92.1	88.2	93.9	90.1	84.0	82.7
G: L=8, d=256, cat	97.5	93.4	85.8	84.7	92.7	81.9	73.9	77.1
H: L=8, d=256, cat&spconv	96.5	89.8	84.5	82.4	89.5	78.2	71.2	74.0
SVT-Net: L=8, d=256, add	97.8	96.5	92.7	90.7	93.7	90.1	84.3	85.5

color, which means they are attended similarly since they may belong to the same object parts. And it can be seen that far away atoms in the 3D space sharing the same implicit mode have similar colors, which means long range contextual information like relationship between semantic similar atoms located in different and far way positions (e.g., the "same-category" information) has been discovered by the model. In the third row, we visualize which token that each non-empty voxel belongs to. Different color represents different tokens. It can be seen that voxels belong to the same token always represent the same objects and share some common geometric characteristics. This observation means that voxels indeed have been clustered together in the feature space according to their geometric characteristics. And obviously, the interaction between clusters or tokens could enhance model's understanding towards the scene. For example, the long range context properties like the relative positions between clusters would be encoded through such kind of interaction. In a word, the visualization results have confirmed our intuition of designing ASVT and CSVT and they have all contributed to the performance improvement.

4.4 Ablation Study

In this section, we study the impact of the number of tokens L , dimension of the final global descriptor d , Transformer feature fusion strategy and training stability of our models. We design experiments from A to H for this study. Table 3 shows the results under different values of L , d and different fusion strategies including adding features (add), concatenating features (cat) and concatenating features followed by SP-Conv (cat&spconv). "SVT-Net" in the last row of Table 3 refers to the model version we finally choose.

Impact of number of tokens: The number of tokens (L) decides how many clusters we divide the scene into. We change the value of L and compare the result in Table 3. Comparing the experiment A, B, C and SVT-Net shows that setting L as 8 is the best choice. When L is too small, interaction is done among only a few tokens, which cannot help our model to fully discover some long range properties between different regions. And when L is too large, it is easy to cause over fitting.

Impact of descriptor dimension: To a certain extent, the dimension d determines the global descriptor's capability of describing a scene. From experiment D, E, F and SVT-Net shown in Table 3, we find that overall larger dimension leads to better performance. However, when it is larger than 256, the increase is minimal while the model size is significantly increase to 1.8M and 3.0M for $d = 384$ and $d = 512$ respectively. Therefore, for a better trade-off between accuracy and model size, we choose $d = 256$ in our implementation.

Impact of fusion strategy: In SVT-Net, we need to fuse features learned by ASVT and CSVT before aggregating voxel features into a global descriptor. In experiment G, we investigate the effectiveness of another fusion method, concatenation. In this way, the output dimension is 512. However, the performance of concatenating the two features is not as good as simply adding them (the dimension is 256). Then, we suspect if it is the higher dimension that causes the performance drop. Therefore, in experiment H, we add an additional SP-Conv layer after concatenation. Unfortunately, the performance of the model becomes even worse than before. Therefore, finally, we believe that direct adding together is the best way to fuse features of the two SVTs.

Training stability: We notice that for each training, there are some small differences on the evaluation results. To avoid bias, we train each model for multiple times and show the boxplot of each model in **supplementary materials**, which reflects the training stability of each model. Considering the trade

off between accuracy, model size, and training stability, we claim that SVT-Net is the best performed model.

5 Conclusions

In this paper, we introduce a super light-weight network for large scale place recognition named SVT-Net. In SVT-Net, two Sparse Voxel Transformers: Atom-based Sparse Voxel Transformer (ASVT) and Cluster-based Sparse Voxel Transformer (CSVN) are proposed to learn long range contextual properties. Extensive experiments have demonstrated that SVT-Net as well as its two simplified versions ASVT-Net and CSVN-Net can achieve state-of-the-art performances with an extremely light-weight network architecture. The limitation is that the current work doesn't consider how to handle complex situation such as when the point cloud is sparse. In the future, we will investigate how to migrate the two proposed Sparse Voxel Transformers into other point cloud based tasks and investigate how to handle more complex scenarios.

References

- [1] Relja Arandjelovic, Petr Gronat, Akihiko Torii, Tomas Pajdla, and Josef Sivic. Netvlad: Cnn architecture for weakly supervised place recognition. In *Proceedings of the IEEE conference on computer vision and pattern recognition*, pages 5297–5307, 2016.
- [2] Herbert Bay, Tinne Tuytelaars, and Luc Van Gool. Surf: Speeded up robust features. In *European conference on computer vision*, pages 404–417. Springer, 2006.
- [3] Chun-Fu Chen, Quanfu Fan, and Rameswar Panda. Crossvit: Cross-attention multi-scale vision transformer for image classification. *arXiv preprint arXiv:2103.14899*, 2021.
- [4] Xieyuanli Chen, Thomas Läbe, Andres Milioto, Timo Röhling, Olga Vysotska, Alexandre Haag, Jens Behley, Cyrill Stachniss, and FKIE Fraunhofer. Overlapnet: Loop closing for lidar-based slam. In *Proc. of Robotics: Science and Systems (RSS)*, 2020.
- [5] Christopher Choy, JunYoung Gwak, and Silvio Savarese. 4d spatio-temporal convnets: Minkowski convolutional neural networks. In *Proceedings of the IEEE/CVF Conference on Computer Vision and Pattern Recognition*, pages 3075–3084, 2019.
- [6] Jacob Devlin, Ming-Wei Chang, Kenton Lee, and Kristina Toutanova. Bert: Pre-training of deep bidirectional transformers for language understanding. *arXiv preprint arXiv:1810.04805*, 2018.
- [7] Alexey Dosovitskiy, Lucas Beyer, Alexander Kolesnikov, Dirk Weissenborn, Xiaohua Zhai, Thomas Unterthiner, Mostafa Dehghani, Matthias Minderer, Georg Heigold, Sylvain Gelly, et al. An image is worth 16x16 words: Transformers for image recognition at scale. *arXiv preprint arXiv:2010.11929*, 2020.
- [8] Zhaoxin Fan, Hongyan Liu, Jun He, Qi Sun, and Xiaoyong Du. Srnet: A 3d scene recognition network using static graph and dense semantic fusion. In *Computer Graphics Forum*, volume 39, pages 301–311. Wiley Online Library, 2020.
- [9] Eduardo Fernández-Moral, Walterio Mayol-Cuevas, Vicente Arevalo, and Javier Gonzalez-Jimenez. Fast place recognition with plane-based maps. In *2013 IEEE International Conference on Robotics and Automation*, pages 2719–2724. IEEE, 2013.
- [10] Dorian Gálvez-López and Juan D Tardos. Bags of binary words for fast place recognition in image sequences. *IEEE Transactions on Robotics*, 28(5):1188–1197, 2012.
- [11] Sorin Grigorescu, Bogdan Trasnea, Tiberiu Cocias, and Gigel Macesanu. A survey of deep learning techniques for autonomous driving. *Journal of Field Robotics*, 37(3):362–386, 2020.
- [12] Meng-Hao Guo, Jun-Xiong Cai, Zheng-Ning Liu, Tai-Jiang Mu, Ralph R Martin, and Shi-Min Hu. Pct: Point cloud transformer. *arXiv preprint arXiv:2012.09688*, 2020.
- [13] Fei Han, Xue Yang, Yiming Deng, Mark Rentschler, Dejun Yang, and Hao Zhang. Sral: Shared representative appearance learning for long-term visual place recognition. *IEEE Robotics and Automation Letters*, 2(2):1172–1179, 2017.
- [14] Kai Han, Yunhe Wang, Hanting Chen, Xinghao Chen, Jianyuan Guo, Zhenhua Liu, Yehui Tang, An Xiao, Chunjing Xu, Yixing Xu, et al. A survey on visual transformer. *arXiv preprint arXiv:2012.12556*, 2020.
- [15] Stephen Hausler, Sourav Garg, Ming Xu, Michael Milford, and Tobias Fischer. Patchnetvlad: Multi-scale fusion of locally-global descriptors for place recognition. *arXiv preprint arXiv:2103.01486*, 2021.

- [16] Jie Hu, Li Shen, and Gang Sun. Squeeze-and-excitation networks. In *Proceedings of the IEEE conference on computer vision and pattern recognition*, pages 7132–7141, 2018.
- [17] Yifan Jiang, Shiyu Chang, and Zhangyang Wang. Transgan: Two transformers can make one strong gan. *arXiv preprint arXiv:2102.07074*, 2021.
- [18] Edward Johns and Guang-Zhong Yang. From images to scenes: Compressing an image cluster into a single scene model for place recognition. In *2011 International Conference on Computer Vision*, pages 874–881. IEEE, 2011.
- [19] Wonjae Kim, Bokyung Son, and Ildoo Kim. Vilt: Vision-and-language transformer without convolution or region supervision. *arXiv preprint arXiv:2102.03334*, 2021.
- [20] Jacek Komorowski. Minkloc3d: Point cloud based large-scale place recognition. In *Proceedings of the IEEE/CVF Winter Conference on Applications of Computer Vision*, pages 1790–1799, 2021.
- [21] Jesse Levinson, Jake Askeland, Jan Becker, Jennifer Dolson, David Held, Soeren Kammel, J Zico Kolter, Dirk Langer, Oliver Pink, Vaughan Pratt, et al. Towards fully autonomous driving: Systems and algorithms. In *2011 IEEE Intelligent Vehicles Symposium (IV)*, pages 163–168. IEEE, 2011.
- [22] Yunpeng Li, Noah Snavely, and Daniel P Huttenlocher. Location recognition using prioritized feature matching. In *European conference on computer vision*, pages 791–804. Springer, 2010.
- [23] Ze Liu, Yutong Lin, Yue Cao, Han Hu, Yixuan Wei, Zheng Zhang, Stephen Lin, and Baining Guo. Swin transformer: Hierarchical vision transformer using shifted windows. *arXiv preprint arXiv:2103.14030*, 2021.
- [24] Zhe Liu, Shunbo Zhou, Chuanzhe Suo, Peng Yin, Wen Chen, Hesheng Wang, Haoang Li, and Yun-Hui Liu. Lpd-net: 3d point cloud learning for large-scale place recognition and environment analysis. In *Proceedings of the IEEE/CVF International Conference on Computer Vision*, pages 2831–2840, 2019.
- [25] David G Lowe. Distinctive image features from scale-invariant keypoints. *International journal of computer vision*, 60(2):91–110, 2004.
- [26] Will Maddern, Geoffrey Pascoe, Chris Linegar, and Paul Newman. 1 year, 1000 km: The oxford robotcar dataset. *The International Journal of Robotics Research*, 36(1):3–15, 2017.
- [27] Raul Mur-Artal, Jose Maria Martinez Montiel, and Juan D Tardos. Orb-slam: a versatile and accurate monocular slam system. *IEEE transactions on robotics*, 31(5):1147–1163, 2015.
- [28] Raul Mur-Artal and Juan D Tardós. Orb-slam2: An open-source slam system for monocular, stereo, and rgb-d cameras. *IEEE Transactions on Robotics*, 33(5):1255–1262, 2017.
- [29] Anish Pandey, Shalini Pandey, and DR Parhi. Mobile robot navigation and obstacle avoidance techniques: A review. *Int Rob Auto J*, 2(3):00022, 2017.
- [30] Adam Paszke, Sam Gross, Francisco Massa, Adam Lerer, James Bradbury, Gregory Chanan, Trevor Killeen, Zeming Lin, Natalia Gimelshein, Luca Antiga, et al. Pytorch: An imperative style, high-performance deep learning library. *arXiv preprint arXiv:1912.01703*, 2019.
- [31] Charles R Qi, Hao Su, Kaichun Mo, and Leonidas J Guibas. Pointnet: Deep learning on point sets for 3d classification and segmentation. In *Proceedings of the IEEE conference on computer vision and pattern recognition*, pages 652–660, 2017.
- [32] Filip Radenović, Giorgos Tolias, and Ondřej Chum. Fine-tuning cnn image retrieval with no human annotation. *IEEE transactions on pattern analysis and machine intelligence*, 41(7):1655–1668, 2018.
- [33] Abhijeet Ravankar, Ankit A Ravankar, Yukinori Kobayashi, Yohei Hoshino, and Chao-Chung Peng. Path smoothing techniques in robot navigation: State-of-the-art, current and future challenges. *Sensors*, 18(9):3170, 2018.
- [34] Ethan Rublee, Vincent Rabaud, Kurt Konolige, and Gary Bradski. Orb: An efficient alternative to sift or surf. In *2011 International conference on computer vision*, pages 2564–2571. Ieee, 2011.
- [35] Qi Sun, Hongyan Liu, Jun He, Zhaoxin Fan, and Xiaoyong Du. Dагc: Employing dual attention and graph convolution for point cloud based place recognition. In *Proceedings of the 2020 International Conference on Multimedia Retrieval*, pages 224–232, 2020.
- [36] Mikaela Angelina Uy and Gim Hee Lee. Pointnetvlad: Deep point cloud based retrieval for large-scale place recognition. In *Proceedings of the IEEE Conference on Computer Vision and Pattern Recognition*, pages 4470–4479, 2018.
- [37] Laurens Van der Maaten and Geoffrey Hinton. Visualizing data using t-sne. *Journal of machine learning research*, 9(11), 2008.

[38] Ashish Vaswani, Noam Shazeer, Niki Parmar, Jakob Uszkoreit, Llion Jones, Aidan N Gomez, Łukasz Kaiser, and Illia Polosukhin. Attention is all you need. *arXiv preprint arXiv:1706.03762*, 2017.

[39] Wenhui Wang, Enze Xie, Xiang Li, Deng-Ping Fan, Kaitao Song, Ding Liang, Tong Lu, Ping Luo, and Ling Shao. Pyramid vision transformer: A versatile backbone for dense prediction without convolutions. *arXiv preprint arXiv:2102.12122*, 2021.

[40] Bichen Wu, Chenfeng Xu, Xiaoliang Dai, Alvin Wan, Peizhao Zhang, Masayoshi Tomizuka, Kurt Keutzer, and Peter Vajda. Visual transformers: Token-based image representation and processing for computer vision. *arXiv preprint arXiv:2006.03677*, 2020.

[41] Yan Xia, Yusheng Xu, Shuang Li, Rui Wang, Juan Du, Daniel Cremers, and Uwe Stilla. Soe-net: A self-attention and orientation encoding network for point cloud based place recognition. *arXiv preprint arXiv:2011.12430*, 2010.

[42] Zhilin Yang, Zihang Dai, Yiming Yang, Jaime Carbonell, Ruslan Salakhutdinov, and Quoc V Le. Xlnet: Generalized autoregressive pretraining for language understanding. *arXiv preprint arXiv:1906.08237*, 2019.

[43] Jun Yu, Chaoyang Zhu, Jian Zhang, Qingming Huang, and Dacheng Tao. Spatial pyramid-enhanced netvlad with weighted triplet loss for place recognition. *IEEE transactions on neural networks and learning systems*, 31(2):661–674, 2019.

[44] Wenxiao Zhang and Chunxia Xiao. Pcan: 3d attention map learning using contextual information for point cloud based retrieval. In *Proceedings of the IEEE/CVF Conference on Computer Vision and Pattern Recognition*, pages 12436–12445, 2019.

[45] Hengshuang Zhao, Li Jiang, Jiaya Jia, Philip Torr, and Vladlen Koltun. Point transformer. *arXiv preprint arXiv:2012.09164*, 2020.

A Appendix

A.1 Results on the refined setting.

Table 4: Comparison with the state-of-the-art methods under the refined setting.

Method	Average recall at top-1% (%)				Average recall at top-1 (%)			
	Oxford	U.S.	R.A.	B.D.	Oxford	U.S.	R.A.	B.D.
PointNetVLAD	80.1	90.1	93.1	86.5	63.3	86.1	82.7	80.1
PCAN	86.4	94.1	92.3	87.0	70.7	83.7	82.3	80.3
DAGC	87.8	94.3	93.4	88.5	71.4	86.3	82.8	81.3
SOE-Net	96.4	97.7	95.9	92.6	89.3	91.8	90.2	89.0
SR-Net	95.3	98.5	93.6	90.8	88.5	93.5	86.8	85.9
LPD-Net	98.2	98.2	94.4	91.6	93.0	90.5	97.4	85.9
Minkloc3D	98.5	99.7	99.3	96.7	94.8	97.2	96.7	94.0
SVT-Net(Ours)	98.4	99.9	99.5	97.2	94.7	97.0	95.2	94.4
ASVT-Net(Ours)	98.3	99.6	98.9	97.0	94.6	97.5	95.0	94.5
CSVT-Net(Ours)	98.6	99.8	98.7	97.3	94.8	96.6	96.2	94.3

For a comprehensive comparison, we show the results of all models at the refined setting in Table 4. We find that at the refined setting, our models still significantly outperform all models except Minkloc3D. In fact, our models still performs better than Minklo3d in most cases, although only by a small margin. The difference between our three models becomes narrow. We attribute this to that all models have reached the performance upper bound. This observation also motivates us to build a more large scale dataset to more fairly evaluate current algorithms and promote future researches. And we leave it as our future work.

A.2 Training stability

We notice that for each training, there are some small differences on the evaluation results. To avoid bias, we train each model for multiple times and show the boxplot of each model in Figure 6, which reflects the training stability of each model. It can be found in the figure that among all settings, the final version of SVT-Net achieves the best trade off between accuracy, model size, and training stability. Therefore, we claim that SVT-Net is the best performed model.

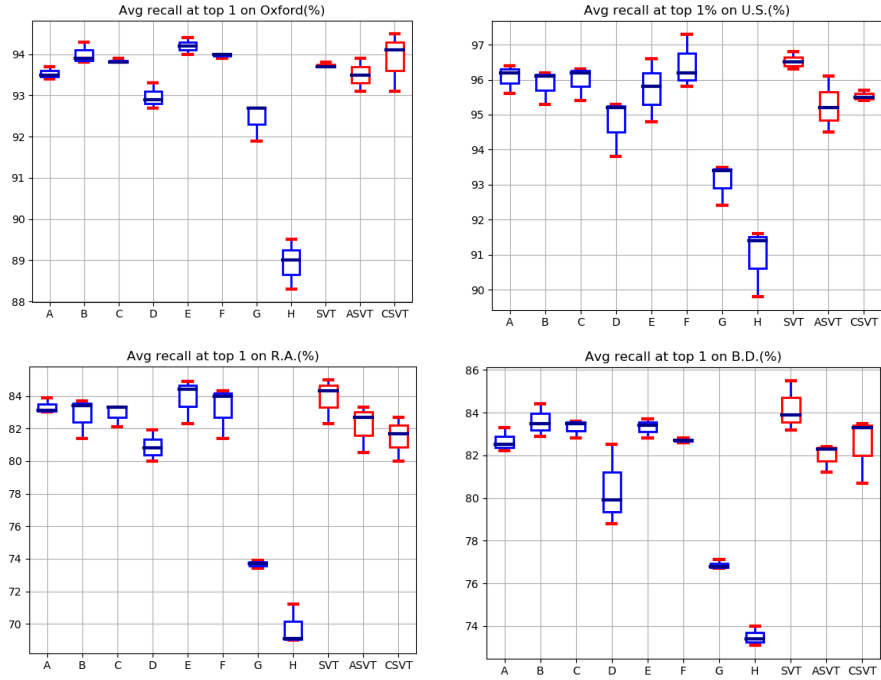


Figure 6: Visualization of training stability.

A.3 Average recall at top N

We show the recall curve of our three models at the baseline setting in Figure 7, which reflects the performance of the models about average recall at top N. It can be found that our three models have already performed very well at top 1. And if we relax the constraints, performance of models largely increase. It demonstrates that our models have the potential of meeting the practical requirements of SLAM systems in terms of accuracy.

A.4 Details about model architecture

We show the detailed information of our model architecture in Table 5. Our SVT-Net takes the sparse voxel representation of a point cloud as input. The input is first processed by a SP-Conv with a kernel size of 5×5 and the stride is 1. Then, two ResNet-like operations are used to learn local features, each operation consists of a 3×3 SP-Conv with stride 2 and a 3×3 SP-Resblock with stride 1. Then a 1×1 SP-Conv is used to lift the feature dimension to 256. Next, ASVT and CSVT are used separately for learning different long range contextual features. Finally, a GeM-Pool is utilized for learning the final descriptor. Parameter numbers of each block are also shown in Table 5. The total parameter number of SVT-Net is about 0.936M.

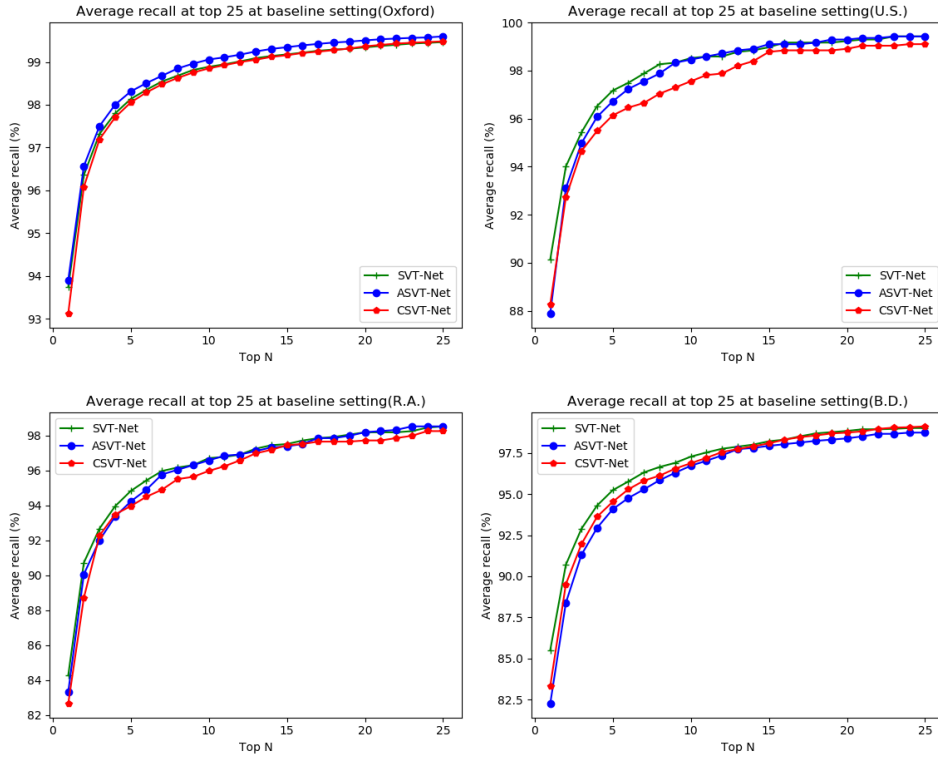


Figure 7: Recall curves of the baseline setting.

Table 5: The SVT-Net Parameters

Blocks & Layers	kernel		channels		# params	input
	size	stride	in	out		
conv0	5	1	3	32	≈ 4.0K	sparse voxel
convs[0]	2	2	32	32	≈ 8.1K	conv0
resblocks[0]	3	1	32	32	≈ 55.4K	convs[0]
convs[1]	3	2	32	32	≈ 8.1K	resblock[0]
resblocks[1]	3	1	32	64	≈ 168.3K	convs[1]
conv1x1	1	1	64	256	≈ 16.3k	resblocks[1]
asvtblocks	1	1	256	256	≈ 147.9K	conv1x1
csvtblocks	1	1	256	256	≈ 526.8K	conv1x1
GeM Pool	-	-	-	-	1	csvtblocks+asvtblocks
Total Parameters	≈ 0.936M					